Simple models to understand some coupling effects in climatology and oceanography

J.I. Díaz

UCM

XIII Escuela *Jacques-Louis Lions* Hispano-Francesa sobre Simulación Numérica en Física e Ingeniería

Valladolid, September, 15-19, 2008

Dedicado a Jacques-Louis Lions,
Admirado y maestro y gran persona.

1. Introduction *Main motivation*.

To show how the S-shaped bifurcation diagrams (arising in climatic Energy Balance Models (EBM)) also arise in some simple models raised in oceanography: the thermohaline circulation model.

Plan:

2. **S shaped bifurcation curves: climatic Energy Balance Models**
3. **S shaped bifurcation curves: a simple thermohaline circulation model**

2. S shaped bifurcation curves: climatic Energy Balance Models

2.1. Some general and previous remarks.

"versus"

Existence and uniqueness of solution	**Existence only for suitable parameters, multiplicity of solutions**

Coercive operators	**Non coercive operators**

Formulation of reaction-diffusion system type:

$$\mathbf{u}_t + \mathbf{Au} = \mathbf{f(u)}, \quad \mathbf{u} : W \ [0, +\infty) \to R^m, \ W \text{open set of } R^n$$

reaction f monotone (dissipative): if m=1 f nonincreasing	**reaction f non monotone: if m=1 f non monotone**

Strong dependence on the boundary conditions

Computational evidences (complex models)	Rigorous proofs (simple models)

A hierarchical set of models

$$\mathbf{u}_t + \mathbf{Au} = \mathbf{f(u)}, \quad \mathbf{u} : W \ [0, +¥ \ ) ® \ R^m, \ W \text{open set of } R^n$$

	n=0	n≥1
m=1	Scalar ODE	Scalar PDE
m≥1	System of ODEs	System of PDEs

Type of solutions (and problems)

Stationary solutions	Periodical solutions	General transient solutions

2.2. A well-known example: the discrete logistic equation.

$$x_{n+1} = l \ x_n (1- \ x_n) = l \ x_n - \ l \ x_n^{\ 2}$$

Coupling: increasing +decreasing

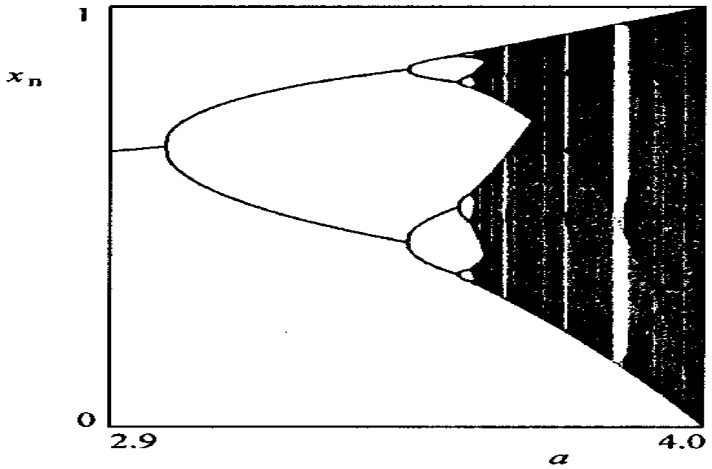

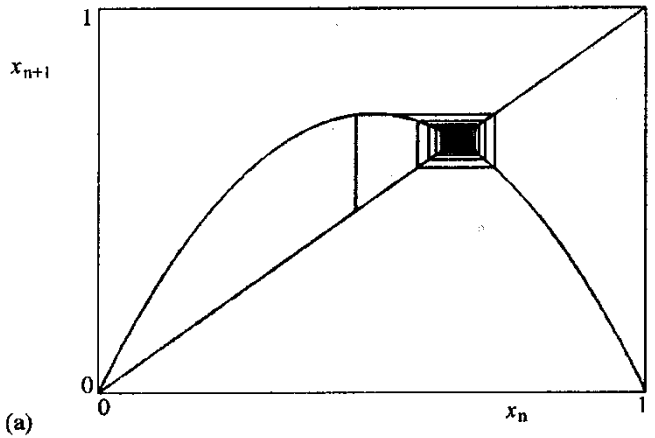

(a)

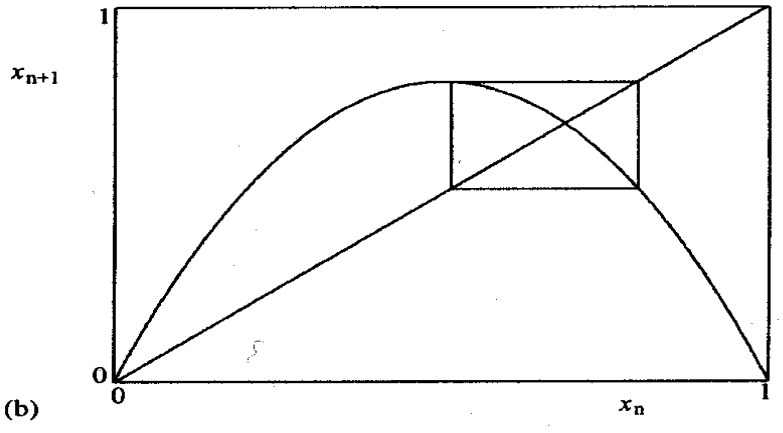

(b)

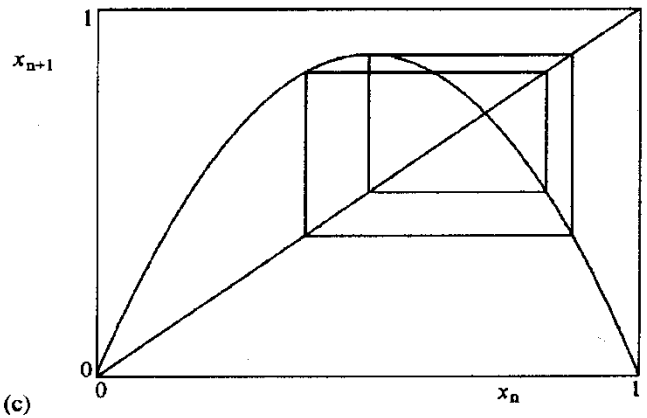

(c)

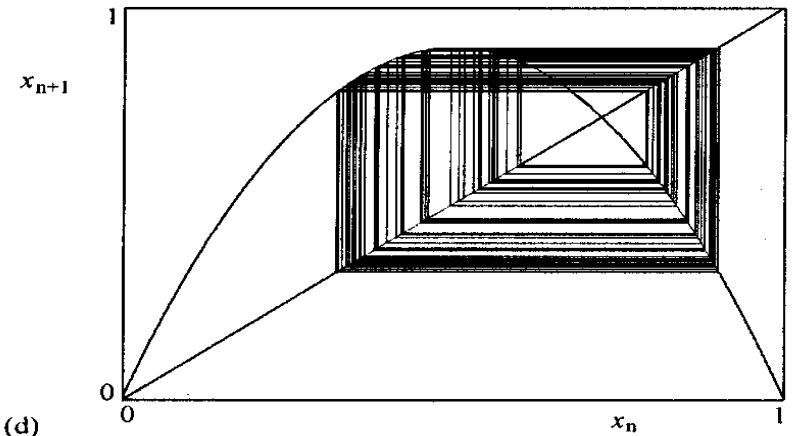

(d)

2.3. S-shaped bifurcation diagrams.

Strict (generalized) S-shaped bifurcation diagram for

$$\mathbf{Au} = \lambda \mathbf{f(u)}, \quad \text{(E)}$$

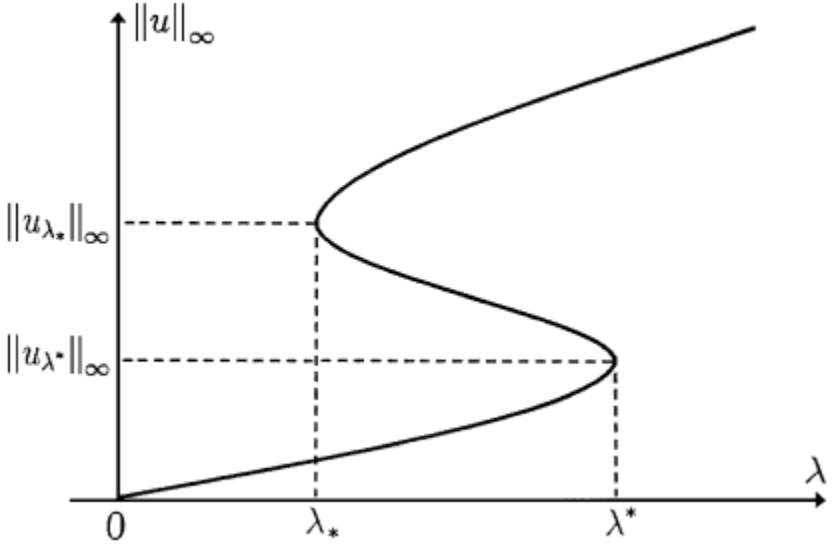

For any given $\alpha > 0$, *there exists a unique (at least)* $\lambda = \lambda(\alpha) > 0$ *such that (E) admits a unique (at least) (positive)* solution *u with* $\|\mathbf{u}\|_\infty = a$ *We define the bifurcation curve of (E) as* $S = \{(\lambda, \|\mathbf{u}\|_\infty)$: $\lambda > 0$ *and u is a positive solution of (E)}.*

The bifurcation curve S is S-shaped in the $(\lambda, \|\mathbf{u}\|_\infty)$ *-plane if S has exactly (at least) two* turning points at some points $(\lambda^*, \|\mathbf{u}^*\|_\infty)$ *and* $(\lambda_*, \|\mathbf{u}_*\|_\infty)$ *such that*

(i) $\lambda^* > \lambda_*$ *and* $\|\mathbf{u}_*\|_\infty \le \|\mathbf{u}^*\|_\infty$

(ii) at $(\lambda^*, \|\mathbf{u}^*\|_\infty)$ *the bifurcation curve S turns to the left,*

(iii) at $(\lambda_*, \|\mathbf{u}_*\|_\infty)$ *the bifurcation curve S turns to the right.*

More precisely, problem (E) has exactly *(at least)* three positive solutions for $\lambda_* < \lambda < \lambda^*$, *exactly two positive solutions* for $\lambda = \lambda_*$ *and* $\lambda = \lambda^*$, *and a unique positive solution for* $0 < \lambda < \lambda_*$ *and* $\lambda^* < \lambda < \infty$.

It appears in many contexts:

- •Nonlinear elasticity (buckling)
- •Combustion theory (Gelfand problem)
- •Social and Human Sciences
- •…

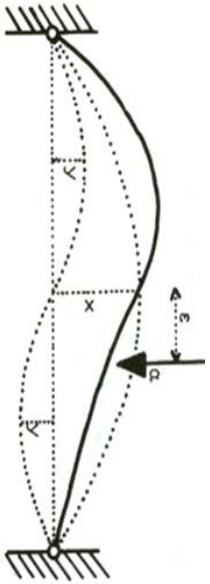

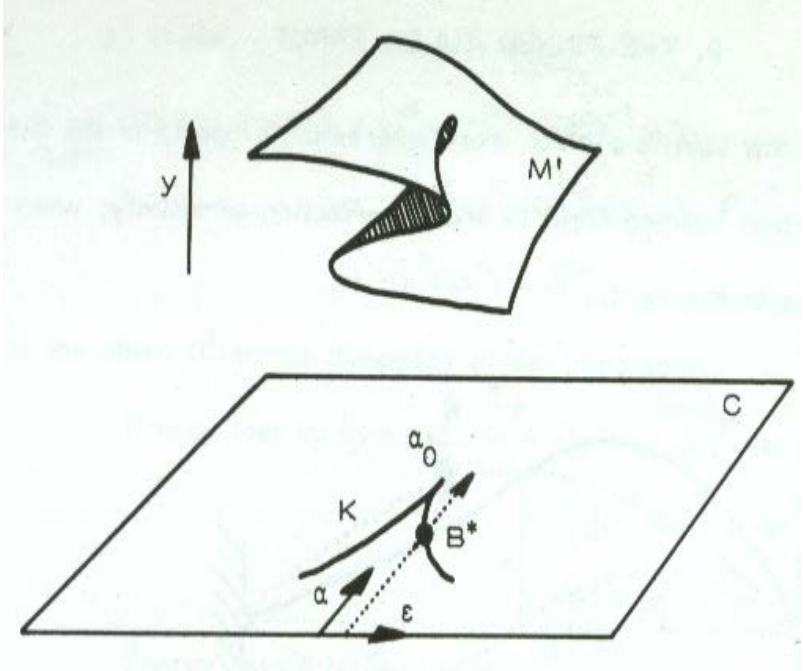

Catastrophe Theory, René Thom,...,

E. C. Zeeman: *Selected papers 1972-1977*

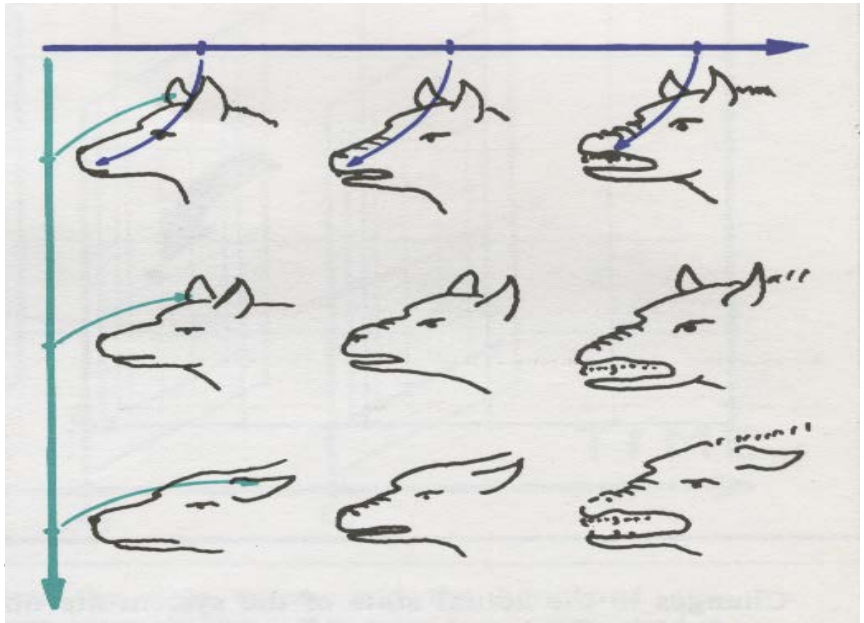

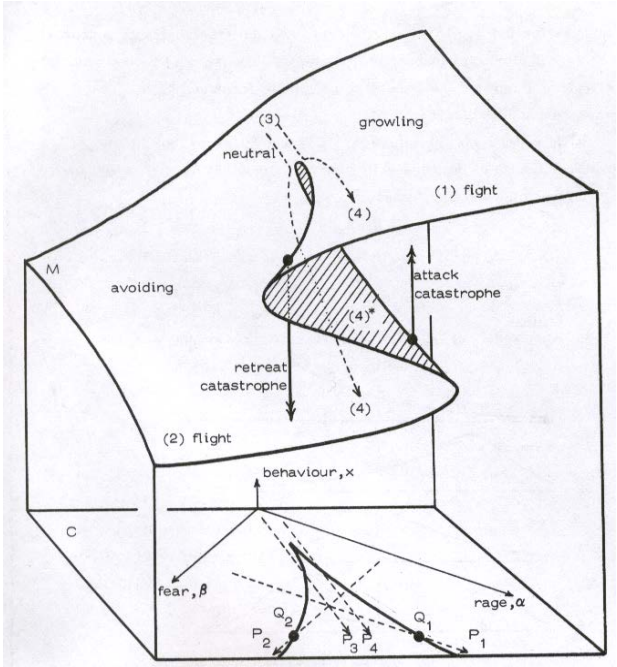

2.4. Bifurcation for Energy Balance Models

XI Escuela Jacques-Louis Lions Hispano-Francesa sobre Simulación Numérica en Física e Ingeniería, Cádiz, 20-24 september, 2004.

R. Dautray, J. I. Díaz: Agir pour conserver l'environnement?: réflexions générales et analyse mathématique de deux problèmes concrets.

In *Apuntes de la XI Escuela Jacques-Louis Lions Hispano-Francesa sobre Simulación Numérica en Física e Ingeniería*, Cádiz, 20-24 septiembre, 2004 (M. Bernardou, F. Ortegón Gallego, eds.), Universidad de Cádiz, Cádiz, 2004, 77-118 (ISBN: 84-688-7650-X).

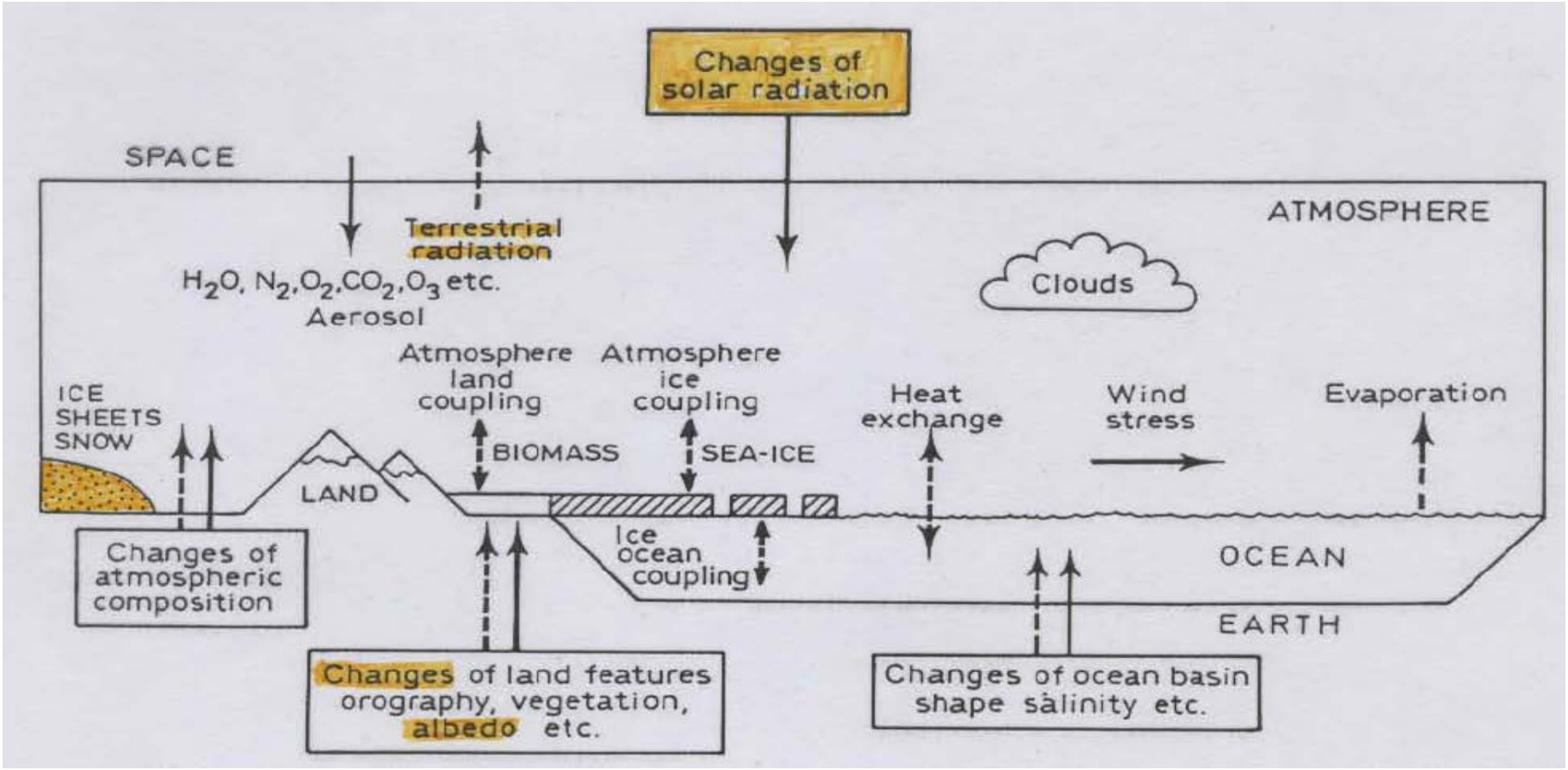

$$c\frac{\partial y}{\partial t} = R_a - R_e + D$$

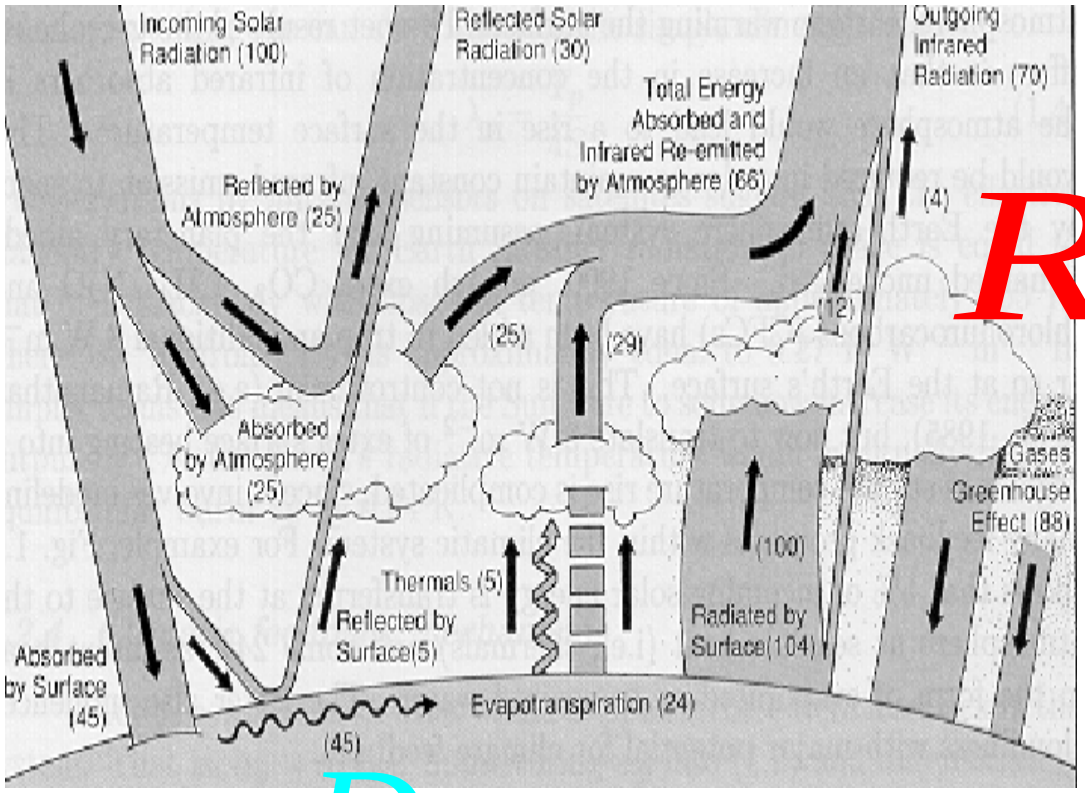

R_e

Greenhouse effect

R_a

Albedo

D

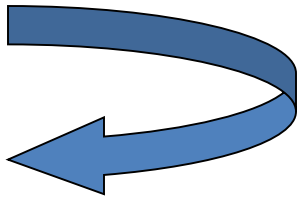

- Pioneer paper: Svante ARRHENIUS (1896)
  On the influence of carbonic acid in the air upon the temperature of the ground, Philosh. Mag, 41, 237-271

- Precursor papers

  W.D. SELLERS (1969) A global climatic model based on the energy balance of the earth-atmosphere system, J. Appl. Meteorol. 8, 392-400

  M.I. BUDYKO (1969) The effects of solar radiation variations on the climate of the Earth, Tellus, 21, 611-619

- simple balance arguments

$$c\frac{\partial u}{\partial t} = R_a - R_e + D$$

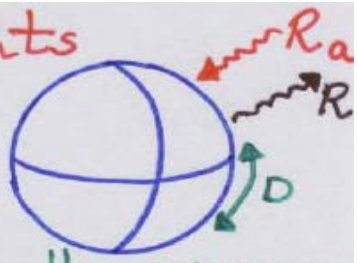

$u(t,x)$:= annually or seasonally averaged surface temperature

c := heat capacity

D := diffusion operator (redistributi

- averaging the atmosphere primitive equations (see e.g. J.T. Kiehl (1992))

Different averaging processes

$$\xi = \xi(t, z, \lambda, \phi)$$

$$\hat{\xi} := \int_0^{z_0} \xi(t,z,\lambda,\phi)\rho\, dz = \int_0^{p_s} \xi(t,p,\lambda,\phi)\frac{dp}{g}$$

$p_s \equiv$ surface pressure

$$[\xi] := \frac{1}{2\pi}\int_0^{2\pi} \xi(t,z,\lambda,\phi)\, d\lambda$$

$$\langle \xi \rangle := \frac{1}{2\pi^2}\int_{-\pi/2}^{\pi/2}\int_0^{2\pi} \xi(t,z,\lambda,\phi)\cos\phi\, d\lambda\, d\phi$$

$$\overline{\xi} := \frac{1}{2\tau}\int_{t-\tau}^{t+\tau} \xi(s,z,\lambda,\phi)\, ds$$

Thermodynamic equation for the atmosphere in flux form

$$c_p\frac{\partial T}{\partial t} = -c_p\nabla\cdot(\vec{v}T) - c_p\frac{\partial(wT)}{\partial p} + c_p\kappa\frac{wT}{p} + \tilde{Q}_{rad} - \tilde{Q}_c$$

$T :=$ temperature [other forms: Lions-Teman-Wang (1992, 93, ...)]

$\vec{v} :=$ horizontal wind vector, w vertical p-velocity

$\kappa := \frac{R}{c_p} \approx 0.286$

$\tilde{Q}_{rad} :=$ net radiative heating

$\tilde{Q}_{con} :=$ heating due to condensational processes

Constitutive laws

$$R_a = QS(x)\beta(u)$$

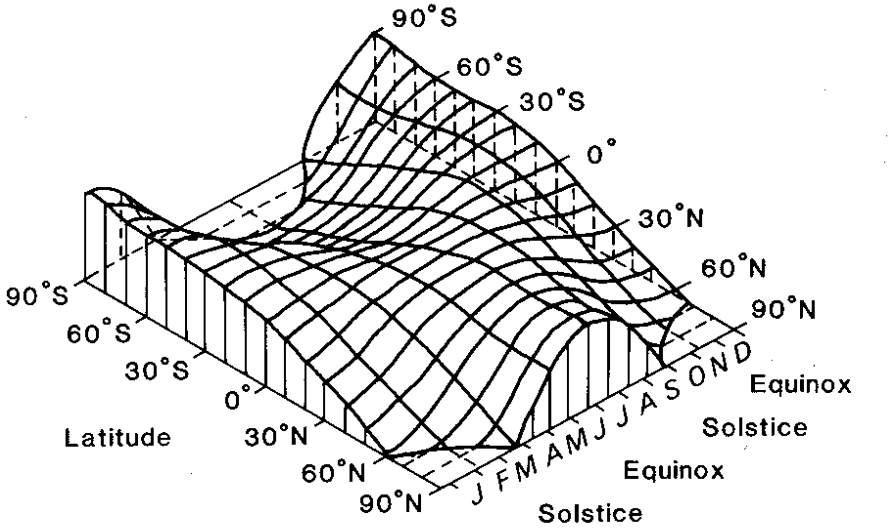

Fig. 2.8. The variation of insolation (at the top of the atmosphere) as a function of

$$\beta(u) = (1 - a(u)) \text{ coalbedo}$$

$$\beta(u) = \begin{matrix} 0.38 \text{ if } u << -10 \\ 0.71 \text{ if } u >> -10 \end{matrix}$$

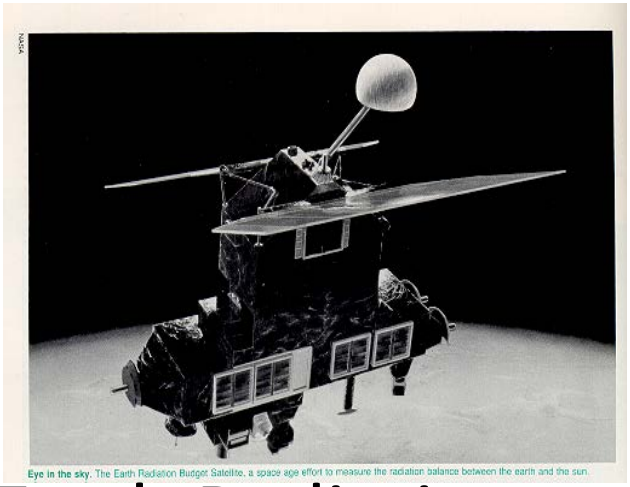
Eye in the sky. The Earth Radiation Budget Satellite, a space age effort to measure the radiation balance between the earth and the sun.

Earth Radiation Budget Satellite

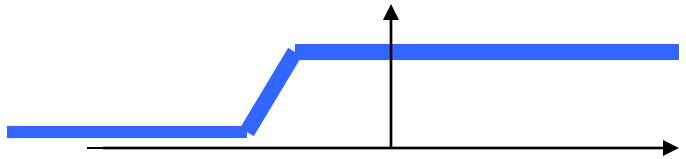

Sellers

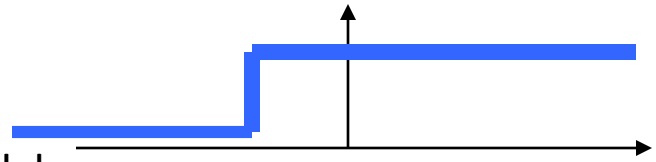

Budyko

On R_e :

Sellers $R_e = \sigma u^4$ Stefan-Boltzman

Budyko $R_e = A + Bu$ Newton

Empirical relation, Depends of the greenhaus gases, anthropogénicos changes,...
(internal variables)

On the diffusion operator, *D*: a hierarchy.

0-dimensional model *D=0*

$$c\frac{du}{dt} = Q\beta(u) - R_e(u)$$

1-dimensional model

$$D = \frac{1}{\cos\varphi}\frac{\partial}{\partial\varphi}\left(k\cos\varphi\frac{\partial u}{\partial\varphi}\right) = \frac{\partial}{\partial x}\left(k(1-x^2)\frac{\partial u}{\partial x}\right)$$

$$x = \cos\varphi$$

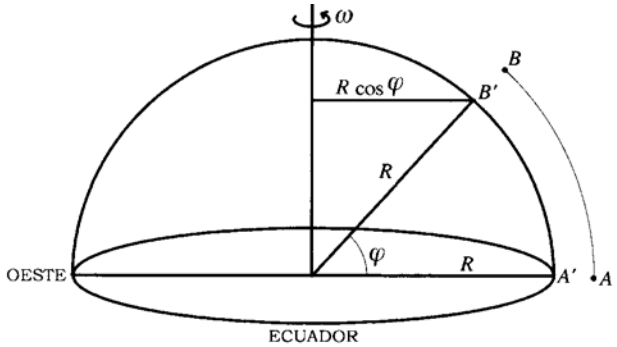

In planetary scales O(10^4 Km) the velocity is eliminated by using the eddy diffusive approximation

Bidimensional model

$$D = div(k(x)\nabla u)$$

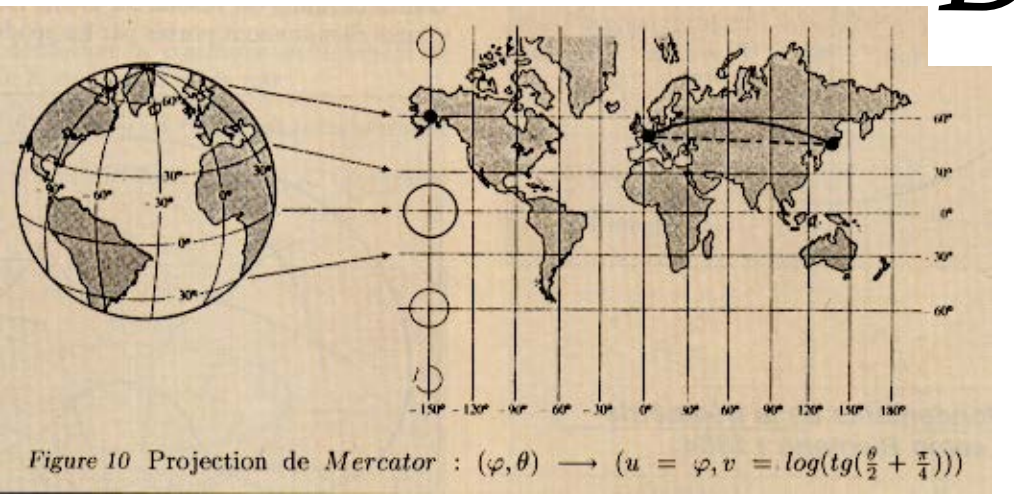

Figure 10 Projection de *Mercator* : $(\varphi, \theta) \longrightarrow (u = \varphi, v = log(tg(\frac{\theta}{2} + \frac{\pi}{4})))$

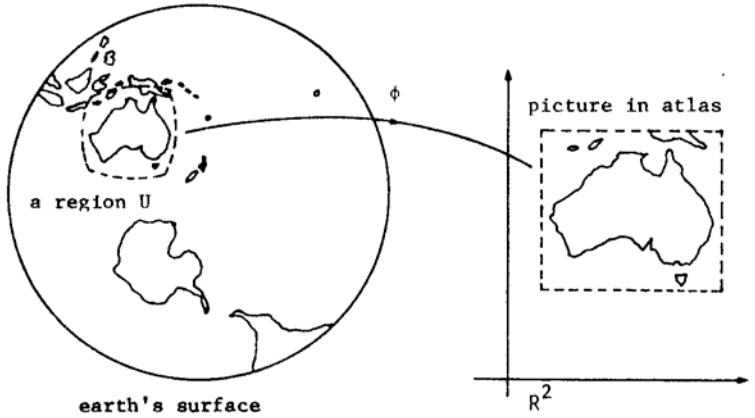

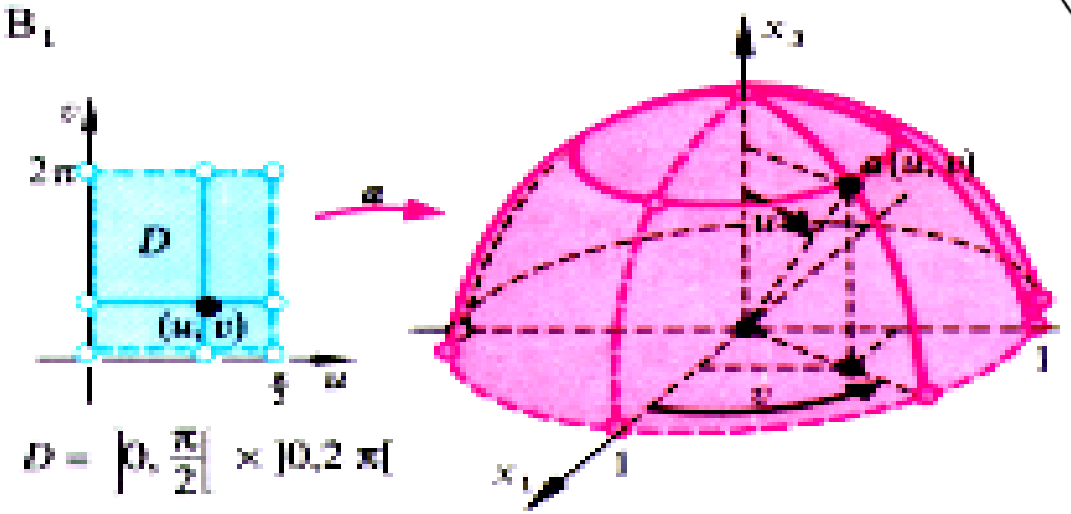

$$D =]0, \frac{\pi}{2}[\times]0, 2\pi[$$

$\sigma : D \longrightarrow \mathbb{R}^3$ déf. par $(u, v) \rightarrow \sigma(u, v)$

$$\sigma(u, v) = \begin{pmatrix} \sin u \cos v \\ \sin u \sin v \\ \cos u \end{pmatrix}$$

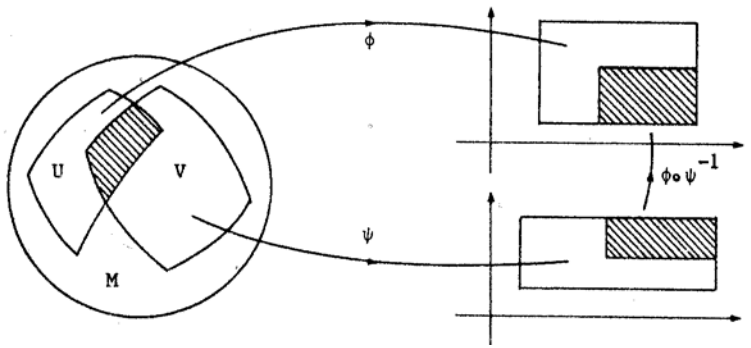

(2a) Recent finite element approach: * R. Bermejo, J. Carpio, J.I. Díaz, P. Galán de Sastre, A finite element algorithm of a nonlinear diffusive climate energy balance model. *Pure and Applied Geophysics*, **165**, nº 6, 2008, 1025-1048.

* R. Bermejo, J. Carpio, J.I. Díaz, L. Tello, Mathematical and Numerical Analysis of a Nonlinear Diffusive Climate Energy Balance Model. To appear in Mathematical and Computer Modelling, 2008.

$$c\frac{\partial y}{\partial t} = Q\beta(y) + R_e(x,y) + div(k(x)\nabla y)$$

First 2d Model: J.I. Díaz and L. Tello, A nonlinear parabolic problem on a Riemannian manifold without boundary arising in Climatology, Collectanea Mathematica 50,1 (1999), 19-51.

Periodic solutions: M. Badii, J. I. Díaz, Time Periodic Solutions for a Diffusive Energy Balance Model in Climatology Journ. Mathematical Analysis and Applications, 233, 713-729, 1999.

$$y(x,t_0) = y_0(x)$$

Some books:

J.I. Díaz and J. L. Lions (eds.), Mathematics, Climate and Environment, Masson, Paris, 1993.

J.I. Díaz and J. L. Lions (eds.), Environment, Economics and Their Mathematical Models, Masson, Paris, 1994.

J.I. Díaz (ed), The Mathematics of Models for Climatology and Environment, NATO ASI Series, Springer Verlag, 1997.

Recent finite element approach: * R. Bermejo, J. Carpio, J.I. Díaz, P. Galán de Sastre, A finite element algorithm of a nonlinear diffusive climate energy balance model. *Pure and Applied Geophysics*, **165**, nº 6, 2008, 1025-1048.

R. Bermejo, J. Carpio, J.I. Díaz, L. Tello, Mathematical and Numerical Analysis of a Nonlinear Diffusive Climate Energy Balance Model. To appear in Mathematical and Computer Modelling, 2008.

First 2d Model: J.I. Díaz and L. Tello, A nonlinear parabolic problem on a Riemannian manifold without boundary arising in Climatology, Collectanea Mathematica 50,1 (1999), 19-51.

Periodic solutions: M. Badii, J. I. Díaz, Time Periodic Solutions for a Diffusive Energy Balance Model in Climatology Journ. Mathematical Analysis and Applications, 233, 713-729, 1999.

2.5. S-shape bifurcation diagrams for the EBM hierarchy

By writing the EBM (eventually coupled with other aspects) we arrive to

$$\mathbf{u}_t + \mathbf{Au} = \mathbf{f(u)}, \quad \mathbf{u}: W\ [0,+\infty) \to R^m, \ W \text{open set of } R^n$$

Results in the literature

	n=0	n≥1
m=1	Scalar ODE (1)	Scalar PDE (2)
m≥1	System of ODEs (3)	System of PDEs (4)

(1) For instance: G.R. North, Multiple solutions in energy balance climate models in *Paleogeography, Paleoclimatology, Paleoecology 82, Elsevier Science Publishers B.V. Amsterdam, 225*-235 (1990).

Bifurcation of stationary states and hysteresis phenomena

Multiple Equilibria for the 0-dimensional EBM

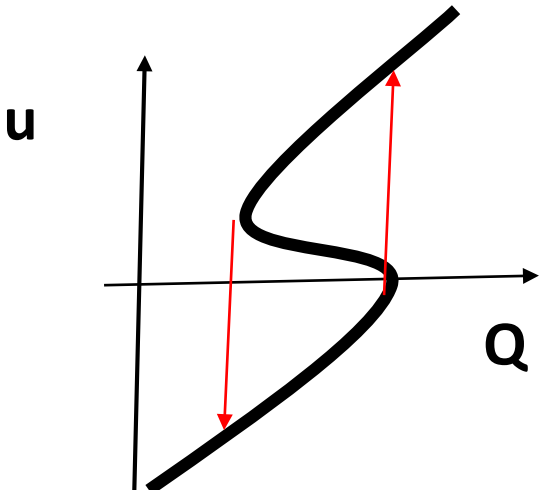

$$A + Bu = Q\beta(u)$$

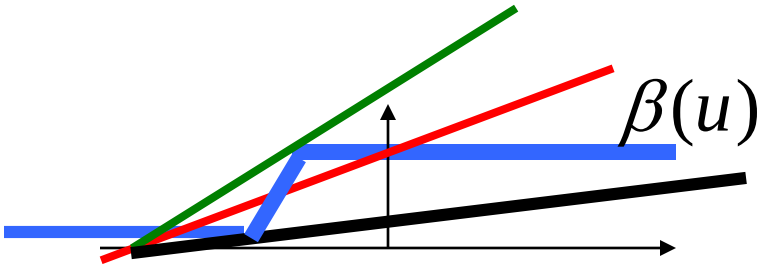

(2b) Bifurcation diagram for EBM:

* J. I. Díaz, J. Hernandez, L. Tello, On the multiplicity of equilibrium solutions to a nonlinear diffusion equation on a manifold arising in Climatology, Journal Mathematical Analysis and Applications, 216, 593-613, 1997

*D. Arcoya, J. I. Díaz, L. Tello, S-Shaped bifurcation branch in a quasilinear multivalued model arising in Climatology, Journal of Differential Equations, 149, 215-225, 1998.

*J. I. Díaz, L. Tello, Infinitely many stationary solutions for a simple climate model via a shooting method, Mathematical Methods in the Applied Sciences, 25, 327-334, 2002.

(2c) Bifurcation diagram for the same type of coupling but related quasilinear equations

J. I. Díaz, J. Hernández and F.J. Mancebo, Branches of positive and free boundary solutions for some singular quasilinear elliptic problems. To appear in Journal of Applied Mathematics and Applications.

$$\mathcal{P}_{\lambda,\alpha} \begin{cases} -(|u'|^{p-2}u')' + \alpha u^m = \lambda u^q \quad \text{in } (-1,1), \\ u(\pm 1) = 0 \end{cases} \qquad -1 < m < q < p-1,$$

For the special case $-\frac{1}{p+1} > m > -1$, $q = 1 + 2m$

the study of the bifurcation diagram is reduced to the application of some properties of the Euler beta function

- Diffusive (stationary) Energy Balance Models

$$P_Q \begin{cases} -\operatorname{div}\left(|\nabla u|^{p-2}\nabla u\right) + G(u) \in Q S(x)\beta(u) + f(x) \\ \qquad\qquad\qquad\qquad\qquad\qquad\qquad\qquad \text{in } M \end{cases}$$

Multiplicity results:

Theorem (D-Hernandez-Tello, 199?)

Assume

(H_S) $S: M \to \mathbb{R}$, $S \in L^\infty(M)$, $S_1 \geq S(x) \geq S_0 > 0$

(H_G^*) $\begin{cases} G: \mathbb{R} \to \mathbb{R} \text{ continuous, strictly increasing, } G(0)=0 \\ \lim_{|s|\to\infty} |G(s)| = +\infty \end{cases}$

a) if $0 < Q < Q_1 \Rightarrow (P_Q)$ has a unique solution

b) if $Q_2 < Q < Q_3 \Rightarrow (P_Q)$ has at least three solutions

c) if $Q_4 < Q \rightarrow (P_Q)$ has a unique solution. ■

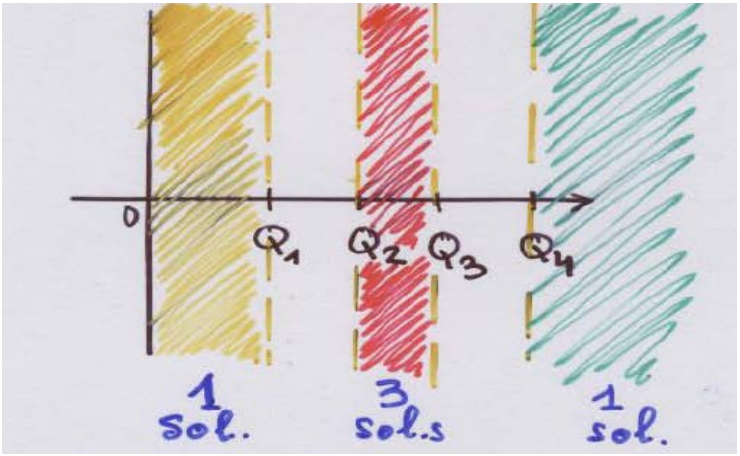

(• Method of super and subsolutions,

• in case (b): construction of two subsolutions (for an approximate equation) V_1, V_2 and two supersolutions U_1, U_2 such that

$$V_2 < U_2 < -10 - \varepsilon < -10 + \varepsilon < V_1 < U_1,$$

Amann theorem (1976) + passing to the limit)

• Sharp results under

(H_f^{**}) $\quad f(x) \equiv C_f$ on M (Budyko's choice)

Bifurcation diagram: Define

$$\Sigma := \{(Q,u) : Q \geq 0 \text{ and } u \text{ is solution of } (P_Q)\}$$

Theorem (Arcoya-D-Tello, 1998)

Σ has an unbounded S-shaped component "starting" in $(0, G^{-1}(-C_f))$ with, at least, two "turning points" contained in the region $(Q_1, Q_2) \times L^\infty(M)$ and $(Q_3, Q_4) \times L^\infty(M)$, respectively.

- Approximate model $\beta \to \beta_\varepsilon$
- Rabinowitz bifurcation theorem (1971)

- Construction of a box

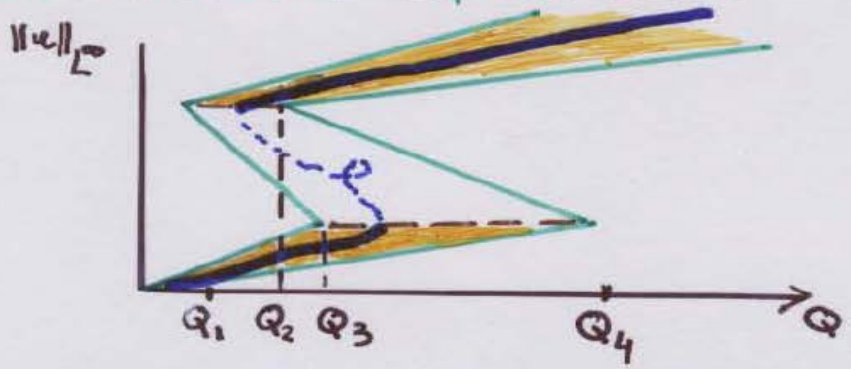

- Passing to the limit by a topological argument (Whyburn 1955)

Remarks

1. Previous results ($p=2$, β regular)

1d - { North (1975), Ghil (1976), ...
Drazin - Griffel (1976), ...
B.E. Schmidt (1996) §

2d { Hetzer (1990), Hetzer - P.L. Schmidt (1990...
North, Mengel, Short (1983), ...

2. Numerical approximation of Σ
Hetzer, Jarausch - Mackens (1989)

Other bifurcation results for the case of systems:

	n=0	n≥1
m=1	Scalar ODE (1)	Scalar PDE (2)
m≥1	System of ODEs (3)	System of PDEs (4)

(3): Bifurcation for a system as spatial discretization of the diffusion operator for EBMs

*J.I. Díaz, V. García, Connecting steady states of a discrete diffusive energy balance climate model XX Congreso de Ecuaciones Diferenciales y Aplicaciones, X Congreso de Matemática Aplicada, *Sevilla, 24-28 septiembre 2007.* Actas electrónicas. Universidad de Sevilla. 2007.

* J.I. Díaz, V. García, Natural and artificially controlled connections among steady states of a climate model Rev. R. Acad. Cien.Serie A Matem, 101 (2), 2007, 229-234.

(4): Bifurcation for systems of EBM type

* G. Hetzer, L. Tello: On a reaction diffusion system arising in Climatology, Dynamical Systems and Applications, Vol. 11, No. 3, 2002, 381-402.

* J. I. Díaz, L. Tello, On a climate model with a dynamic nonlinear diffusive boundary condition, Discrete and Continuous Dynamical Systems series S, Vol 1, N. 2, (2008), 253-262.

2.6. Bifurcation and control: J.-L-Lions.

Lecture at the Collège de France Seminar: May 1997.

J. I. Díaz

Diffusive energy balance models in climatology

En *Nonlinear Partial Differential Equations and their Applications*, Collège de France Seminar, Volume XIV, D. Cioranescu and J.L.Lions eds., North-Holland, Amsterdam,.2002, 297-328, ISBN:0-444-51103-2

COL.DE FRANCE No FAX:33-1-44271704 2 JUN 97 17:50 No.010 P.

mathématiques peuvent apporter :

- le contrôle local (facile)
- la possibilité de contrôle à plus grande échelle

Contrôle de turbulence — Contrôle des configurations

- pour les très grandes échelles, la première position est celle du

Contrôle des bifurcations.

C'est ce dernier point qui a attiré mon attention dans ton (très bon) exposé au Collège de France car tu as un modèle "pas trop complexe", qui est lié à la climatologie, et qui exhibe des bifurcations.

C'est donc ici mais très intéressant Conceptuellement - j'ai déjà dans plusieurs de mes travaux antérieurs jamais sans vraiment y croire - là il y a quelque chose.

Merci n'oublie pas de m'envoyer les copies de tes transparents de ta conf. au Collège.

Fax émis par : + 33 01 44 41 44 28 ACAD SCIENCES PARIS 17/06/97 13:46 Pg: 1/7

— 1 —

COLLÈGE DE FRANCE
J.-L. LIONS
Président de l'Académie des Sciences

Paris, le 17/6

FAX Prof. J. DIAZ.

Mardi Eldefonso

Merci beaucoup pour ta lettre du 6 mai et tes commentaires et remarques. Je me suis un peu cassé la tête à distance. Oh la la ... .

1. Considérons

$$(1) \qquad \frac{\partial y}{\partial t} - \Delta y + \beta(y) = \alpha S(x) A(y) + f_\infty(x) + v(x) \gamma_\infty$$

1ère difficulté

Si on introduit un contrôle $v \neq 0$ la notion de solution stationnaire devient ... contrôlable.

Donc considérons d'abord comme toi le cas $v = 0$. et le diagramme de bifurcation connu dans ton Fax

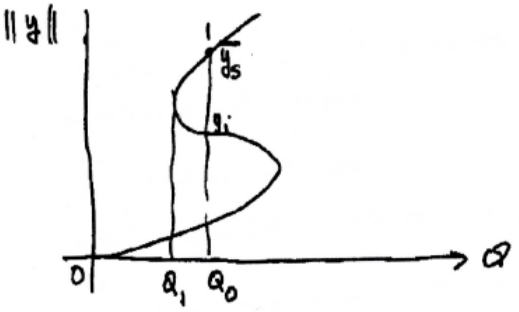

Contester

- Enunciar el Pb de von Neuman
- Contestar $y_0 = y_i$
- $g \in L^\infty$ ∃
- variar Q (Noticias mucho fructífero)
- VIL (citar reacciones químicas)
- Modelos simples de EL Niño y controlabilidad (2)

Joint papers on some different problems with multiple solutions (and blow up in a finite time)

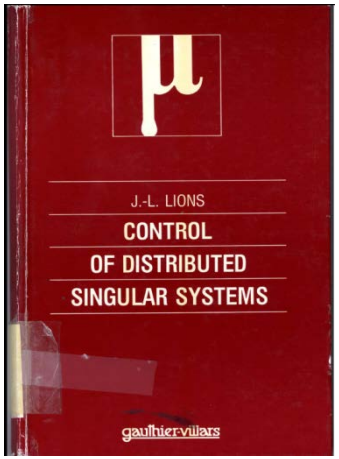

Previous treatment:

J.-L. Lions, *Control of Distributed Singular Systems*, Gauthier-Villars, Paris (1985).

J. I. Díaz, J.-L. Lions, Sur la contrôlabilté approchée de problèmes paraboliques avec phénomènes d'explosion, Comptes Rendus Acad. Sci. Paris, t. 327, Série I, 173-177, 1998.

J. I. Díaz, J. -L. Lions
On the approximate controllability for some explosive parabolic problems
International Series of Numerical Mathematics, Vol. 133, Birkhäuser Verlag, Basel, pp. 115-132, 1999.

Other collaborations:

J. I. Díaz, J. -L. Lions
On the Approximate Controllability of Stackelberg-Nash Strategies. In, *Ocean Circulation and Pollution Control. A Mathematical and Numerical Inquiry*, (J. I. Díaz ed.). Lecture Notes, EMS Volume, Proceedings of the Diderot Videoconference Amsterdam-Madrid-Venice, Lecture-Notes, Springer Verlag 2003, 17-28.

J. I. Díaz, J. -L. Lions: El planeta Tierra (Second edition): unfinished.

3. S shaped bifurcation curves: a simple thermohaline circulation model

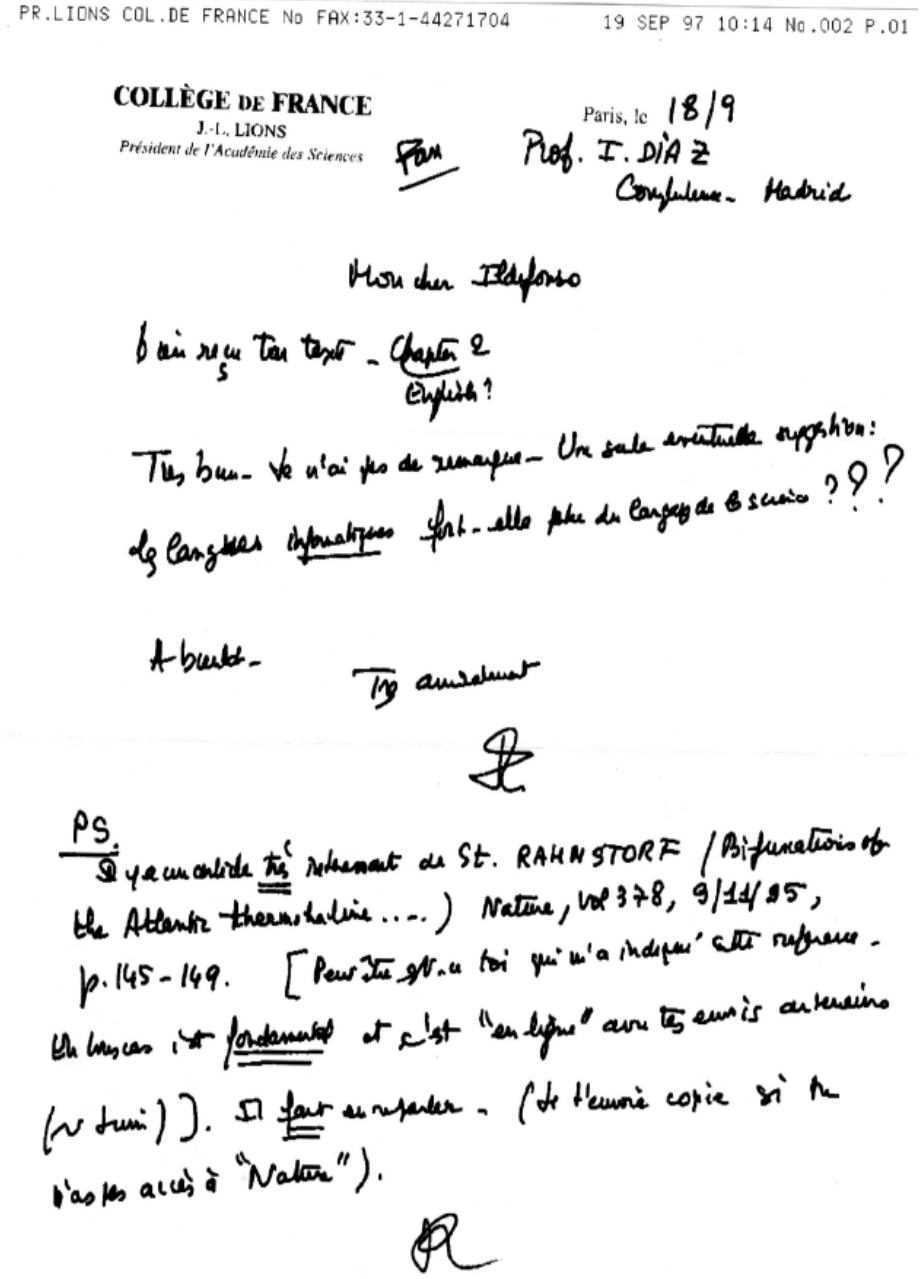

PR.LIONS COL.DE FRANCE No FAX:33-1-44271704 19 SEP 97 10:14 No.002 P.01

COLLÈGE DE FRANCE
J.-L. LIONS
Président de l'Académie des Sciences

Paris, le 18/9

Fax Prof. I. DIAZ
Complutense Madrid

Mon cher Ildefonso

J'ai reçu ton texte - Chapter 2
English?

Très bien - Je n'ai pas de remarque - Une seule éventuelle suggestion:
les Conditions Initiales font-elles partie du Concept de Solution ??

A bientôt -

Ton ami

PS
Il y a un article très intéressant de St. RAHMSTORF / Bifurcations of the Atlantic thermohaline ....) Nature, Vol 378, 9/11/95, p. 145-149. [Peut-être as-tu toi qui m'a indiqué cette référence - Un travail très fondamental et c'est "en ligne" avec tes amis américains (Courant)]. Il faut en reparler - (Je t'envoie copie si tu n'as pas accès à "Nature").

Personal interest on the topic since 1997.

S. Rahmstorf, Bifurcations of the Atlantic thermohaline circulation in response to changes in the hydrological cycle. *Nature* **378**, (1995) 145-149.

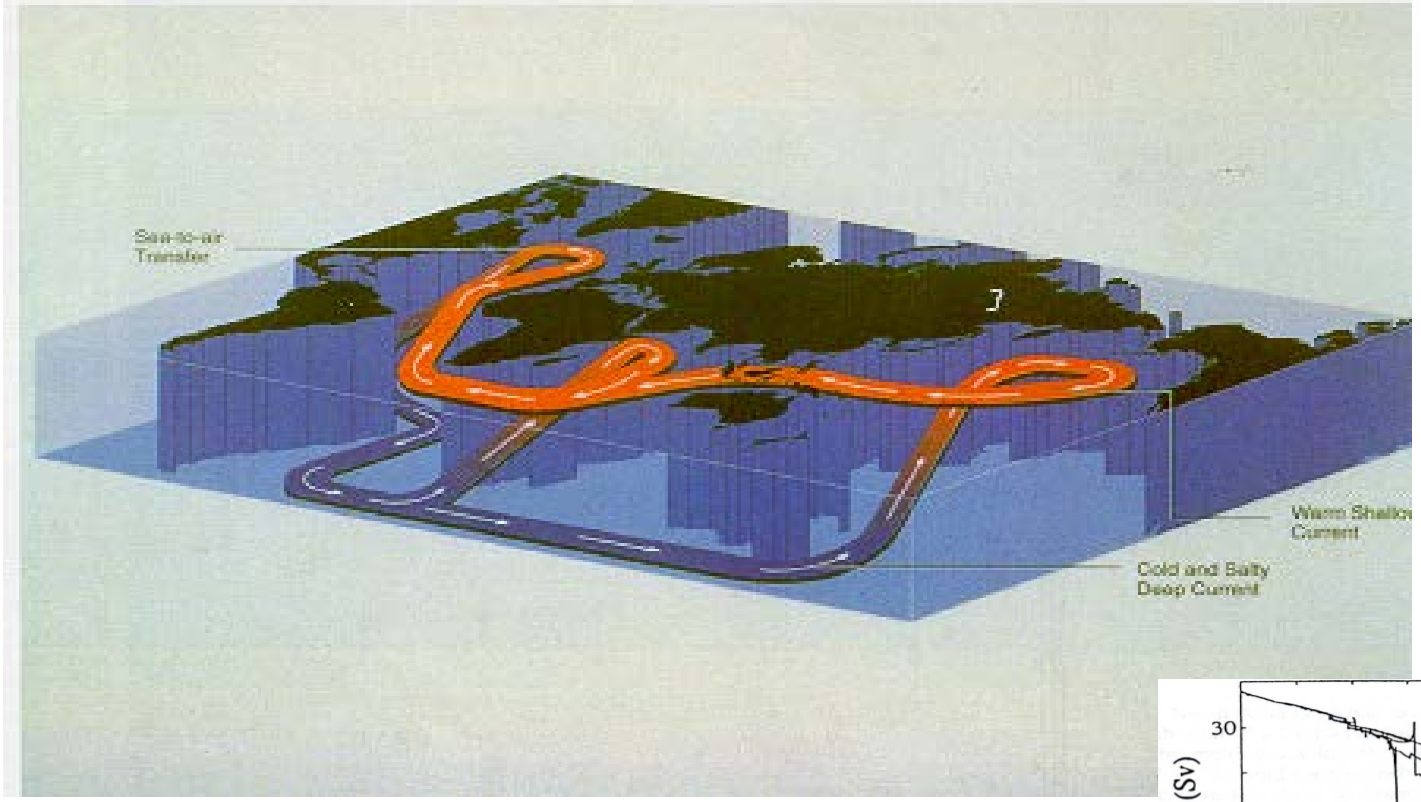

Question: sensitivity of the North Athantic thermohaline circulation to the imput of fresh water:

Global ocean circulation model coupled to a simplified model atmosphere

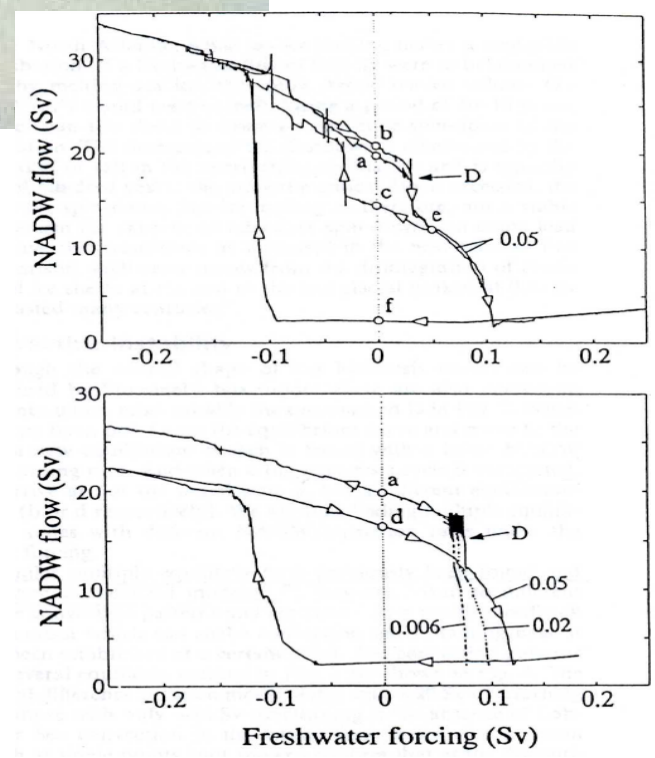

Confirmation of the multiple states results for a simplified model:

Stommel, H., 1961: Thermohaline convection with two stable regimes of flow. *Tellus,* ***13, 224-230.***

$$\frac{dT}{dt} = c(\mathcal{T} - T)$$

$$\frac{dS}{dt} = d(\mathcal{S} - S)$$

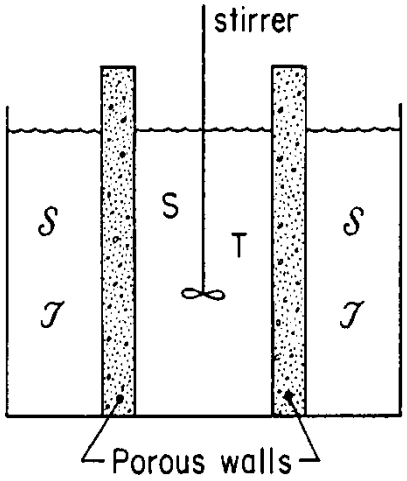

Here we shall give a “rigorous proof” to the S-shaped bifurcation diagram for a model generalizing the Stommel model

Marotzke, J. and Willebrand: Multiple equilibria of the Global Thermohaline Circulation , *Journal of Physical Oceanography*, **21**, 1991, 1372-1385.

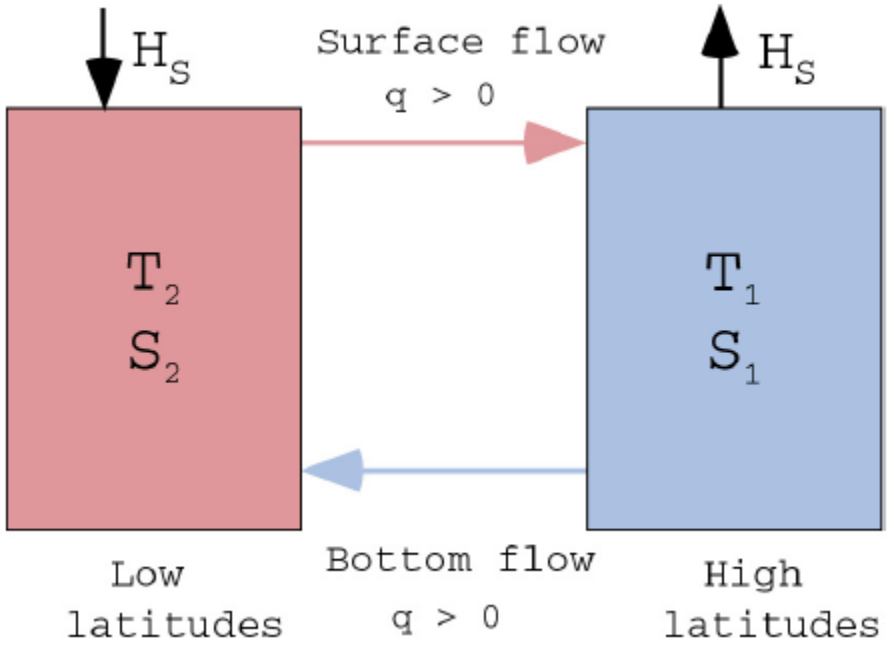

We assume that the atmosphere controls the ocean temperature and the surface fresh-water loss or gain, E (in m/s). For now, let us proceed with the assumption that T1 , T2 , and E are prescribed as external parameters

we will use a virtual surface salinity flux,

$$H_S = S_0 E/D$$

where D is depth and S_0 a reference salinity.

The boxes are connected by pipes near the surface and the bottom; the pipes are assumed to have vanishing volume but are conduits for the flow. The thermohaline circulation strength is denoted by q (strictly speaking, q represents THC/Volume; q has units of s^{-1}). We use the sign convention that q>0 denotes poleward surface flow, implying equatorward bottom flow and, conceptually, sinking at high latitudes. This is the picture that we are used to when thinking about the North Atlantic THC. Conversely, q<0 means equatorward surface flow and poleward bottom flow. We assume a very simple flow law for q, namely, that it depends linearly on the density difference between high and low latitudes:

$$q = \frac{k}{\rho_0}[\rho_1 - \rho_2]$$

where ρ_0 is a reference density and k is a hydraulic constant, which contains all dynamics, that is, the connection between density and the flow field. The equation of state is

$$\rho_i = \rho_0 (1 - \alpha T_i + \beta S_i);\ i = 1, 2\ ,$$

where α and β are, respectively, the thermal and haline expansion coefficients,

$$\alpha \equiv -(1/\rho_0)\partial_T \rho \quad \beta \equiv (1/\rho_0)\partial_S \rho \,.$$

For simplicity, we employ a linear equation of state; that is, both α and β are assumed constant. The flow law, (2), thus becomes, using (3),

$$q = k\left[\alpha(T_2 - T_1) - \beta(S_2 - S_1)\right]$$

As we assume that the temperatures are fixed by the atmosphere and enter the problem as external parameters, we need not formulate a heat conservation equation. The salt conservation equations for the Stommel model are

$$\dot{S}_1 = -H_S + |q|(S_2 - S_1)\,,$$

$$\dot{S}_2 = H_S - |q|(S_2 - S_1)\,,$$

We introduce the following abbreviations for meridional differences of temperature, salinity, and density:

$$T \equiv T_2 - T_1; \quad S \equiv S_2 - S_1; \quad \rho \equiv \rho_1 - \rho_2 ,$$

which implies that

$$q = \frac{k}{\rho_0}\rho = k\left[\alpha T - \beta S\right].$$

Under normal conditions, net evaporation occurs at the warmer low latitudes and net precipitation at the colder high latitudes; in other words, temperature and salinity are expected to be both high at low latitudes and both low at high latitudes. In their influence on the THC, two cases can be distinguished. When the temperature difference dominates the salinity difference in their influence on density, high-latitude density is greater than the low-latitude density.

Therefore, q>0, and the surface flow is poleward. One can say that the temperature difference, T, drives the THC and the salinity difference, S, brakes the THC, as seen from

$$q > 0 : \left|q\right| = q = k\left[\alpha T - \beta S\right].$$

Conversely, when the salinity difference dominates the temperature difference, highlatitude density is lower than the low-latitude density, q<0, the surface flow is equatorward. Now, S drives the THC, and T brakes it:

$$q < 0 : |q| = -q = k[\beta S - \alpha T]$$

The sum of the salt conservation equations (6) and (7) gives

$$\dot{S}_1 + \dot{S}_2 = 0 ,$$

reflecting that total salt mass is conserved. (One consequence of this simplification is that we cannot determine the mean salinity from the set of equations we use here. Processes other than evaporation, precipitation, and oceanic transport of salinity must be invoked for the determination of the total oceanic salt content.) Because of the constancy of total salt mass, (12), equivalent to the constancy of global mean salinity, we need only consider the difference, S, between S2 and S1. The difference of the salt conservation equations (6) and (7) gives an equation for S:

$$\dot{S}_2 - \dot{S}_1 = \dot{S} = 2H_S - 2|q|S ,$$

or, using the flow law

$$\dot{S} = 2H_S - 2k|\alpha T - \beta S|S ,$$

which completes the formulation of the model – its behaviour is completely characterised by (14) .

Equilibrium solutions

As the first step in our analysis of (14), governing the evolution of the salinity difference between the low and high latitude boxes, we look for steady-state or equilibrium solutions, defined by a vanishing of the time derivative:

$$H_S - k\left|\alpha T - \beta \overline{S}\right| \overline{S} = 0\,,$$

where the overbar marks a steady-state quantity. We must consider separately the cases where the argument of the modulus is positive or negative.

Case I:

$$\overline{q} > 0, \quad \alpha T > \beta \overline{S}$$

We can simply replace the modulus signs by brackets, giving

$$H_S - k\left(\alpha T - \beta \overline{S}\right) \overline{S} = 0\,,$$

or

$$\left(\beta \overline{S}\right)^2 - \left(\beta \overline{S}\right)(\alpha T) + \beta H_S / k = 0\,,$$

which has the roots

$$\left(\beta \overline{S}\right)_{1/2} = (\alpha T)\left\{\tfrac{1}{2} \pm \sqrt{\tfrac{1}{4} - \frac{\beta H_S}{k(\alpha T)^2}}\right\}.$$

For a positive radicand, defined by

$$\frac{\beta H_S}{k(\alpha T)^2} < \tfrac{1}{4},$$

the model has two equilibrium solutions for poleward near-surface flow. These solutions can also be characterized as thermally dominated or, in the language of atmospheric science, “thermally direct” (meaning that rising motion occurs at the location of heating, and subsidence at the location of cooling). If the freshwater flux forcing exceeds the threshold defined by (20), no thermally-driven equilibrium exists.

Case II:

$$\overline{q} < 0, \quad \alpha T < \beta \overline{S}$$

Now, we must insert a minus sign when replacing the modulus signs by brackets,

$$H_S + k\left(\alpha T - \beta \overline{S}\right)\overline{S} = 0,$$

which gives

$$\left(\beta \overline{S}\right)^2 - \left(\beta \overline{S}\right)(\alpha T) - \beta H_S / k = 0,$$

and the single root

$$\left(\beta \overline{S}\right)_3 = (\alpha T)\left\{\tfrac{1}{2} + \sqrt{\tfrac{1}{4} + \frac{\beta H_S}{k(\alpha T)^2}}\right\}$$

Notice that we must discard the negative root; the radicand is greater than ¼, so that the negative
root would imply *S < 0, in contradiction to the condition (10.21). The solution (10.24) has* equatorward near-surface flow and can be characterised as salinity dominated or “thermally indirect”. It exists for all (positive) values of the freshwater flux forcing.
Figure 10.2 shows the equilibrium solutions as a function of the freshwater flux forcing.
In summary, we find the remarkable result that this simplest non-trivial model of the THC, represented in steady state by the pair of quadratic equations, (10.15) and (10.22), has three steady state solutions, provided that the freshwater flux forcing is not too strong [cf., (10.20)].
Two equilibria have *q > 0 (poleward surface flow); they are characterised by either a small* salinity contrast and strong flow (1 1
2 2 β*S<αT,q> kαT), or by a large salinity contrast and*
weak flow (1 12 2 β*S>αT,q< kαT). These steady states exist only if*
( )214*HSk T*βα < . The model

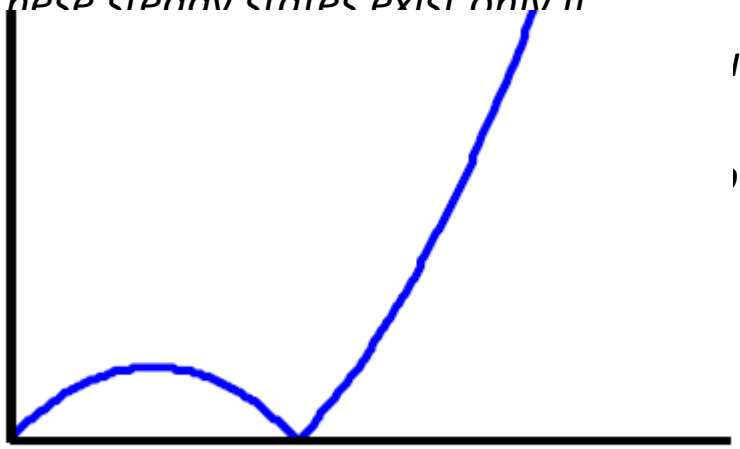

ıatorward surface flow), characterised by a very
salinity contrast (β*S>αT,q<0).* *ıne if*
( )214*HSk T*βα > .

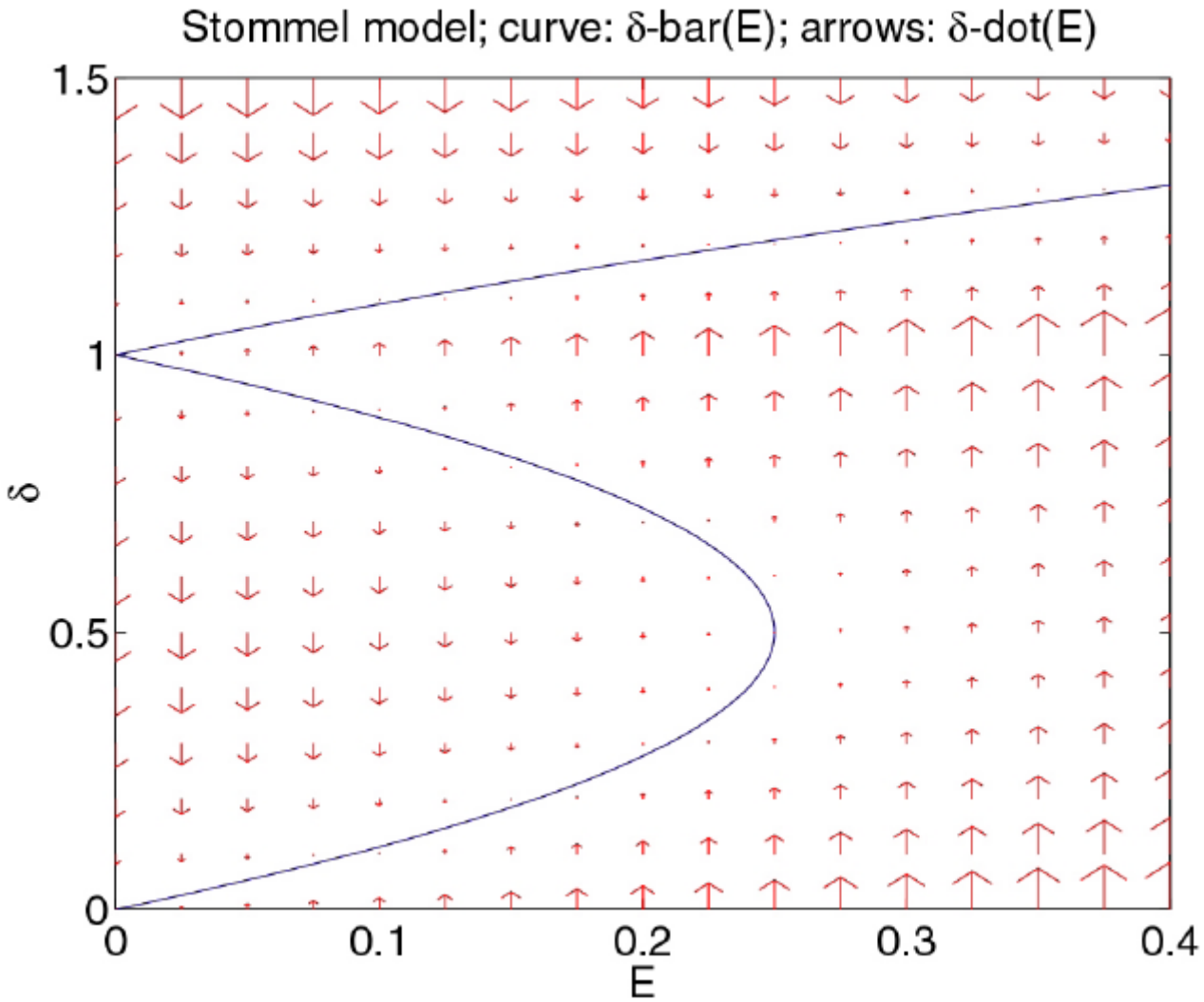
Stommel model; curve: δ-bar(E); arrows: δ-dot(E)
1.5
1
0.5
0
δ
0
0.1
0.2
0.3
0.4
E

Solution portrait of the box model in phase space. Dimensionless salinity difference is denoted δ ≡ β*SαT; dimensionless surface salinity flux is ( )2 S E≡βH kαT .*The curves mark the equilibrium solutions, δ (*E), while the arrows show the tendencies in* phase space. Notice the existence of three steady states for E < ¼.

What is the physical reason behind the vanishing of the thermally direct solution if ( )2α > ? Stronger surface salinity flux must by balanced by stronger salinity advection, qS. This can be accomplished either by increasing the salinity difference, S, between low and high latitudes, or by increasing the flow strength, q. But increasing S has the dynamical consequence
of weakening the flow – (9) expresses that q decreases linearly with S. Obviously, the product, qS, is zero for either S = 0 or q = 0 (the latter implying β*S=αT); qS is positive for* intermediate values and attains a maximum at 1
2 β*S= αT (see phase space diagram, Fig. 2).* At this point, ( )2*, which marks the critical freshwater flux forcing, that is, the* strongest forcing that can be balanced by salinity advection through thermally direct flow. For even greater HS, balance is impossible.

An even deeper question than the one starting the preceding paragraph is, what makes the multiple equilibria possible in the first place? Two crucial ingredients are required. First is theadvective nonlinearity: The flow advecting salinity is itself influenced by salinity gradients, through density. Without this nonlinearity the model would have a unique solution (or none atall). But there is a second requirement, that of different coupling of temperature and salinity to the atmosphere. We assume that the atmosphere controls temperature but the salinity *flux.*

Imagine, instead, two extreme cases of equal coupling:

i. Temperature ***and salinity prescribed:***

Then, density is prescribed as well, meaning that the flow prescribed. Trivially, no multiple equilibria are possible.

ii. Heat ***and freshwater flux prescribed:***

Then, the surface density (or buoyancy) flux is prescribed and, hence, the steady-state horizontal density transport, *k ρ ρ . As k and ρ are positive, the sign ofρ is uniquely* determined by the sign of the surface buoyancy flux: If the low latitude box receives buoyancy from the atmosphere, it is less dense than the high latitude box, andρ and *q are both positive* (thermally direct circulation). The converse is true for prescribed buoyancy loss at low latitudes. Hence, the steady-state circulation is uniquely determined.

Stability

We have identified three equilibria of the 2-box model of the THC in a certain parameter range. Now, we concern ourselves with the stability of the equilibria – more precisely, with the "linear" stability. This means that we want to understand what happens if the equilibrium is perturbed by a tiny amount, either in the forcing, HS, or in the solution, S. We will use a variety of techniques, each of which is important generally in the analysis of dynamical systems, and each of which illuminates one or several characteristics.

We start by investigating in more detail the equilibrium curves in phase space, Fig. 10.2. From the steady-state conditions, as expressed in eqs. (10.18) and (10.23), we obtain through a slight modification,

$$\overline{q} > 0, \frac{\beta \overline{S}}{\alpha T} < 1: \quad \frac{\beta H_S}{k(\alpha T)^2} = -\left(\frac{\beta \overline{S}}{\alpha T}\right)^2 + \left(\frac{\beta \overline{S}}{\alpha T}\right),$$

$$\overline{q} < 0, \frac{\beta \overline{S}}{\alpha T} > 1: \quad \frac{\beta H_S}{k(\alpha T)^2} = +\left(\frac{\beta \overline{S}}{\alpha T}\right)^2 - \left(\frac{\beta \overline{S}}{\alpha T}\right),$$

which expresses the dimensionless salinity gradient, δ ≡β*SαT, as a function of the* dimensionless surface salinity flux, ( )2
S E≡ϐH kαT . Thus, we can write (10.29) and (10.30)in dimensionless form as

$$\delta \le 1: \quad E = -\delta^2 + \delta = \delta(1-\delta)$$

$$\delta \ge 1: \quad E = \delta^2 - \delta = \delta(\delta - 1).$$

This pair of equations represents two sideways parabolas, with opposite orientation, intersecting at δ≡β*SαT=0 (no salinity difference) and δ =1 (αT=ϐS; no flow). In either case, the* forcing must vanish (( )2 0 *S E≡ϐH kαT =). The curves depicted in Fig. 10.2 are the zeros of* the salinity conservation equation (10.14), rewritten in dimensionless form as

$$\frac{1}{2k\alpha T}\frac{d}{dt}\left(\frac{\beta S}{\alpha T}\right) = \frac{\beta H_S}{k(\alpha T)^2} - \left|1 - \left(\frac{\beta S}{\alpha T}\right)\right|\left(\frac{\beta S}{\alpha T}\right).$$

Notice that (10.33) implies an advective timescale, suitable for nondimensionalisation, of ( )1 2*kαT − , and a nondimensional overturning strength of q=1−δ . We can thus rewrite*

$$\dot{\delta} = E - |1-\delta|\delta$$

From either (10.33) or (10.34), we can read off the following. On the equilibrium curve, the tendency (time rate of change) of the salinity difference between high and low latitudes vanishes. But to the left of the curve, E or HS is smaller than required by the equilibrium condition. Hence, *S < 0 , and S decreases, as indicated by the downward pointing arrows in Fig.*10.2. In fact, the arrows were calculated from the right-hand sides of (10.34). To the right of the curve, E or HS is greater than required for equilibrium, hence *S > 0 , and S increases. Notice that* for every given δ in Fig. 10.2, there belongs a unique E, so “left” and “right” of the equilibrium curve are unambiguously defined. By

By visual inspection of Fig. 10.2, we can now read off the stability properties of the solutions. If, by any initial perturbation or change in forcing, we find ourselves to the left of the equilibrium curve, the evolution depends critically on which solution branch we started from. On the top ($\delta > 1$) and bottom ($\delta < 1$ 2) branches in Fig. 10.2 (salinity dominated and thermally dominated-strong flow, respectively), the systems moves downward, back towards the equilibrium curve. But if one starts from the middle branch ($1\ 2 < \delta < 1$), which runs from topleft to bottom-right in Fig. 10.2, the system does not return, but instead undergoes a transition towards the lower, thermally dominated branch. If the initial perturbation or change in forcing leaves the system to the right of the equilibrium curve, the system moves upward, again back towards the equilibrium curve, if it started from the top or the bottom branch. But if it started from the middle branch, it would make a transition toward the salinity-dominated equilibrium.

Hence we conclude that the salinity-dominated steady state is always stable, the strong-flow thermally dominated steady state is stable (if it exists), while the weak-flow thermally dominated steady state is unstable to infinitesimal perturbations. There exists a tell-tale sign allowing one to infer this instability even without investigating the full time-dependent equation. As one follows the unstable branch in Fig. 10.2 ($1\ 2 < \delta < 1$), from left to right, say, an increase in E implies a decrease in δ. Thus, an *increase in forcing leads to a decrease in the steady-state response, which* is, to my knowledge, an unfailing indication of instability.

Two points deserve special mention, since they are *semistable, meaning that the system* approaches them if it is on one side in phase space, but moves away from them if it is on the other side. These points are (*E=0, δ=1), where the two parabolas meet, and* (*E=1 4, δ=1 2), the point beyond which no thermally direct steady state is possible. (In the* language of dynamical systems, this is called a saddle node bifurcation.) Both these points show interesting mathematical behaviour, but they are not of great physical interest because this behaviour is not robust to small perturbations, such as a small amount of random noise.

Lyapunov potential

A powerful illustration of the stability properties discussed in the preceding paragraphs comes from a mathematical construct called the "Lyapunov potential". In loose analogy to, say, the relationship between gravitational force and gravitational potential, the time rate of change of dimensionless salinity, δ , (cf., (10.34)), is written as the negative gradient of the Lyapunov potential, L, such that

$$-\frac{\partial L}{\partial \delta} = \dot{\delta} = E - |1-\delta|\,\delta\,.$$

By construction, the steady states of the system coincide with the extrema (maximum or minimum) of the Lyapunov potential. But we can say more: Plotting *L(δ) immediately indicates*the stability properties of the equilibria; indeed one can interpret the stability as if a bead was sliding on a wire under the influence of gravity: A minimum in L is a stable equilibrium, while a maximum is an unstable equilibrium. We first illustrate this graphically, before showing it mathematically.

It is readily shown that

$$L = -E\delta - \tfrac{1}{3}\delta^3 + \tfrac{1}{2}\delta^2; \qquad \delta \le 1$$

$$L = -E\delta + \tfrac{1}{3}\delta^3 - \tfrac{1}{2}\delta^2 + \tfrac{1}{3}; \qquad \delta \ge 1$$

fulfils (10.35), including the (arbitrary) condition of *L(0) = 0 and the (non-arbitrary) condition* of continuity at δ =1. Figure 10.3 shows the Lyapunov potential, as a function of δ, for a variety of choices for E. The case, *E = 0 , has one minimum at δ = 0 and a double extremum (level* turning point) at δ =1. The former is stable, according to Fig. 10.2, while the latter is semistable (approached from the right, moved away from on the left). Thus, we can visualise the evolution of the system as the inertia-less sliding of a bead on the "wire" *L(δ). As E is nonzero but less* than ¼, the minimum at the left moves from zero to higher values, while another minimum appears for δ >1 and growing. Since *L(δ) is continuous, the two minima must be separated by* a maximum. In other words, two stable equilibria must have an unstable equilibrium between them.

As E approaches ¼, the minimum at δ >1 becomes deeper than the one at δ <1 2, until, at *E =1 4, the two equilibria with δ <1 merge to form a level turning point. This is the second* semistable point discussed in Fig. 10.2. For even greater E, the thermally dominated (δ <1) equilibrium vanishes altogether, although its vicinity can still be felt through the very small time rates of change nearby.

After gaining an intuitive understanding of how to interpret *L, we can now derive* mathematically how its shape reflects stability properties. At any point, if *L increases with δ, the*left-hand side of (10.35) is negative, $\delta < 0$, and δ decreases. In the *L(δ) phase plot, Fig. 10.3,* one slides toward the left. The converse is true if L decreases with δ. In the vicinity of a minimum, hence, any deviation to the right (*L increasing with δ) is followed by motion to the* left, back toward the minimum. Likewise, any deviation to the left will be followed by motion back to the minimum. Near a maximum, instead, a deviation to the right, say, means that *L decreases with δ, the left-hand side of (10.35) is positive,* $\delta > 0$ *, and δ increases further, that is,* the system moves further to the right, away from the equilibrium. For deviations to the left of a maximum, $\delta < 0$, and δ decreases further, again moving away from the equilibrium. Hence, if we can construct a Lyapunov potential as in (10.36), we can immediately read off the plot the stable and unstable steady states, in a completely intuitive manner.

Notice that in a case such as depicted in Fig. 10.3, sometimes the nomenclature is adopted to call the stable equilibrium with the shallower potential well “metastable”, reserving the term “stable” only for the steady state with the globally lowest potential. Here, we will largely only concern ourselves with distinguishing between stability and instability to infinitesimal perturbations.

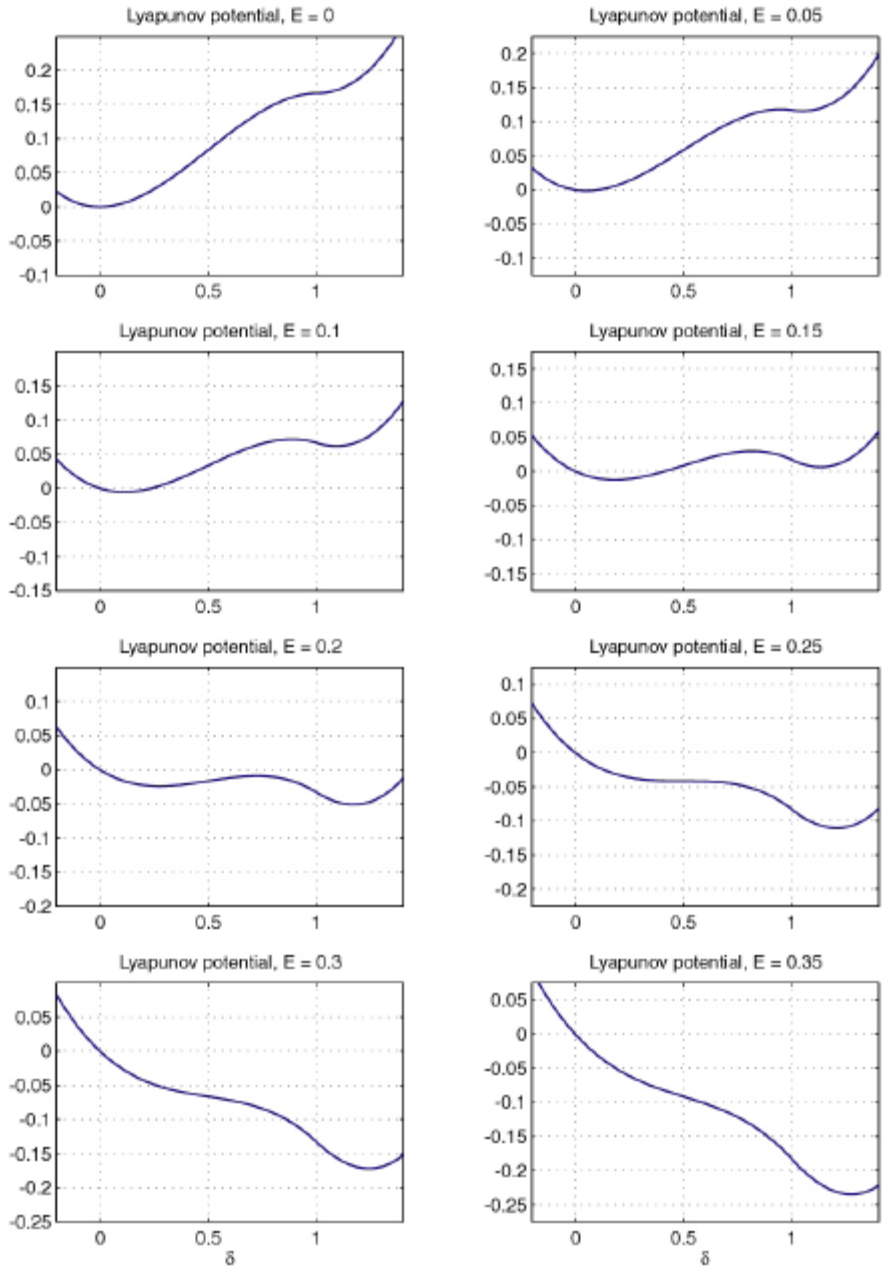
Lyapunov potential, E = 0
Lyapunov potential, E = 0.05
Lyapunov potential, E = 0.1
Lyapunov potential, E = 0.15
Lyapunov potential, E = 0.2
Lyapunov potential, E = 0.25
Lyapunov potential, E = 0.3
Lyapunov potential, E = 0.35
δ
δ